Supplementary Material

for

Deep Immune Profiling of MIS-C demonstrates marked but transient immune activation compared to adult and pediatric COVID-19

Vella, Giles, Baxter, Oldridge *et al*

Supplementary Figure Legends

SUPPLEMENTAL FIGURE LEGENDS

Supplemental Figure 1 - Innate immune compartment in MIS-C is broadly comparable to Pediatric COVID-19

(**A**) White blood cell (WBC) counts in pediatric cohorts at time of draw. (**B**) Clinically determined cell counts in pediatric cohorts at time of draw. (**C**) Gating strategy and representative flow cytometry plots for immune populations from whole blood stain. (**D**) Frequencies of eosinophils, neutrophils and immature granulocytes across all cohorts. (**E**) Monocyte and subset frequencies across all cohorts. (**F**) Dendritic cell (DC) and subset frequencies across all cohorts. (**ABDEF**) Each dot represents an individual patient or subject, with adult HD in grey circles, adult COVID-19 in shades of mauve indicated by disease severity score, Ped COVID-19 in blue circles, with ARDS patients in dark blue, and MIS-C in green triangles. (**AB**) Normal clinical laboratory reference ranges for healthy pediatric subjects are indicated in grey shading. (**DFE**) Significance determined by unpaired Wilcoxon test between Ped COVID-19 and MIS-C groups only, indicated by: * $p<0.05$, or P value shown.

Supplemental Figure 2 - T cell proliferation in MIS-C is greater than in COVID-19

(**A**) Gating scheme and representative flow cytometry plots for CD4 and CD8 T cell populations, from PBMC staining. (**B**) Frequencies of nonnaive(nn) CD4 T cell memory populations. (**C**) Frequencies of nnCD8 T cell memory populations. (**D**) Representative flow cytometry plots and quantification of Ki67+ nnCD4 T cells. (**E**) Representative flow cytometry plots and quantification of Ki67+ nnCD4 T cells. (**F**) Distribution of T cell memory subsets within HLA-DR+CD38+ nnCD4 (left) and CD8 T cells (right). (**G**) Distribution of T cell memory subsets within Ki67+ nnCD4 (left) and CD8 T cells (right). (**B-G**) Each dot represents an individual patient or subject, with adult HD in grey circles, adult COVID-19 in shades of mauve indicated by disease severity score, Ped COVID-19 in blue circles, with ARDS patients in dark blue, and MIS-C in green

triangles. (**BCDE**) Significance determined by unpaired Wilcoxon test between Ped COVID-19 and MIS-C groups only, indicated by: ** p<0.01, or P value shown.

Supplemental Figure 3 - NK and CD8 MAIT cell activation in MIS-C is greater than in COVID-19

(**A**) Representative flow cytometry plots and quantification of HLA-DR and CD38 single and double-expressing NK cells from the whole blood panel. (**B**) Representative flow cytometry plots and quantification of HLA-DR and CD38 single and double-expressing CD8 MAIT from the whole blood panel. (**AB**) Each dot represents an individual patient or subject, with adult HD in grey circles, adult COVID-19 in shades of mauve indicated by disease severity score, Ped COVID-19 in blue circles, with ARDS patients in dark blue, and MIS-C in green triangles. Significance determined by unpaired Wilcoxon test between Ped COVID-19 and MIS-C groups only, indicated by: * p<0.05, or P value shown.

Supplemental Figure 4 - Vascular patrolling CX3CR1+ populations in MIS-C are uniquely proliferative in MIS-C

(**A**) Quantification of Ki67+ population within CX3CR1- and CX3CR1+ nnCD4 T cells. (**B**) Quantification of Ki67+ population within CX3CR1- and CX3CR1+ nnCD8 T cells. (**C**) Representative gating of Ki67+ population within CX3CR1- and CX3CR1+ nnCD8 T cells. (**AB**) Each dot represents an individual patient or subject, with adult HD in grey circles, adult COVID-19 in shades of mauve indicated by disease severity score, Ped COVID-19 in blue circles, with ARDS patients in dark blue, and MIS-C in green triangles. Significance determined by unpaired Wilcoxon test between Ped COVID-19 and MIS-C groups and determined by paired Wilcoxon test between CX3CR1- and CX3CR1+ within pediatric groups, indicated by: * p <0.05, ** p<0.01, *** p<0.001 or P value shown.

Supplemental Figure 5 - A transition towards B cell memory subsets from naive is associated with IFNg in both MIS-C and pediatric COVID-19

(**A**) Representative gating for naive B cells and memory subsets. (**B**) Frequencies of naive B cells. (**C**) Frequencies of memory B cell subsets from the nonnaive(nn)B cell population. (**D**) Spearman correlation for indicated cytokines with frequencies of B cell subsets. Top panel indicates correlations in the combined pediatric cohort, lower two panels represent correlations within the Ped COVID-19 and MIS-C respectively. Spearman's Rank Correlation coefficient (ρ) is indicated by square size and heat scale; significance indicated by: * $p<0.05$, ** $p<0.01$, *** $p<0.001$. (**E**) Spearman correlation for indicated cytokines with frequencies with HLA-DR+CD38+ and Ki67+ populations of nnCD4 and nnCD8 T cells, statistics and panels as in **D**. (**F**) Representative histogram of Eomes expression by PB for an adult HD (grey), Ped COVID-19 (blue) and MIS-C (green) and quantification of frequencies of Eomes+ PB. Significance determined by unpaired Wilcoxon test between pediatric cohorts indicated by: **** $p<0.001$.

Supplemental Figure 6 - Total and activated cTfh frequencies are not associated with PB responses in either pediatric cohort.

(**A**) Representative flow cytometry plot and quantification for cTfh. (**B**) Representative flow cytometry plot and quantification for activated cTfh. (**CDE**) Frequencies of PB versus cTfh from nnCD4 T cells (**C**), activated cTfh from nnCD4 T cells (**D**), activated cTfh from total cTfh (**E**). Non-parametric trend lines (Sen-Theil) with Spearman’s Rank Correlation coefficient (ρ) and associated P value shown. (**F**) Representative flow cytometry plot and quantification for both frequency of CXCR5+ nnCD4 T cells and CXCR5 GMFI on nnCD4 T cells. Significance determined by unpaired Wilcoxon test comparing adult HD to both pediatric cohorts and indicated by: * $p<0.05$, ** $p<0.01$, *** $p<0.001$ or P value shown. (**A-F**) Each dot represents an individual patient or subject, with adult HD in grey circles, adult COVID in shades of mauve indicated by disease severity score, Ped COVID-19 in blue circles, with ARDS patients in dark

blue, and MIS-C in green triangles. (**AB**) Significance determined by unpaired Wilcoxon test between pediatric cohorts.

Supplemental Figure 7 - Features of CD4 T cell activation start to normalize over time, coincident with treatment and recovery from disease.

(**A**) Selected CD4 T cell features over days since admission in Ped COVID-19 (left) and MIS-C subjects (right). Black lines connect repeat draws for individual subjects. For MIS-C, paired t-test P value is shown for the three subjects with repeat draws. Grey shading indicates the derived central 95% adult HD reference interval. (**B**) Flow cytometry plots for HLA-DR+CD38+ nnCD4 for MIS-C patients with repeat draws. (**C**) Flow cytometry plots for Ki67+ nnCD4 for MIS-C patients, as in (**B**). (**A**) Each dot represents an individual patient with Pediatric COVID-19 in blue circles (ARDS patients in dark blue) and MIS-C in green triangles.

	Pediatric COVID-19		MIS-C	
Demographics	**Value (% or Range)***	**N****	**Value (% or Range)***	**N****
Age (Years)	14 [0.15-18]	16	9 [5.00-17]	14
Sex (F/M)	8 (50%) / 8 (50%)	16	7 (50%) / 7 (50%)	14
BMI (Age-Matched Percentile)	65 [1-99]	16	92 [5-99]	14
Race (African-American/Caucasian)	8 (53%) / 7 (47%)	15	4 (31%) / 9 (69%)	13
Medical History				
Obesity	2 (12%)	16	5 (36%)	14
Diabetes Mellitus	1 (6%)	16	0 (0%)	14
Symptomatic	13 (81%)	16	14 (100%)	14
Coinfection	5 (31%)	16	1 (7%)	14
Disease Type (COVID-19 non-ARDS / COVID-19 with ARDS / MIS-C)	12 (75%) / 4 (25%) / 0 (0%)	16	0 (0%) / 0 (0%) / 14 (100%)	14
Treatment				
Hydroxychloroquine	1 (6%)	16	0 (0%)	14
Remdesevir	4 (29%)	14	1 (11%)	9
Convalescent Plasma	2 (12%)	16	0 (0%)	14
Tociluzimab	3 (19%)	16	0 (0%)	14
Vasoactive Medication	8 (50%)	16	9 (64%)	14
Intravenous Immunoglobulin	1 (6%)	16	14 (100%)	14
Intravenous Immunoglobulin Before First Draw Date	0 (0%)	1	11 (79%)	14
Steroids	6 (38%)	16	13 (93%)	14
Steroids Before First Draw Date	6 (100%)	6	10 (77%)	13
Laboratory Results				
Hemoglobin, 1st Research Draw	10.3 [7.4-14.8]	15	9.3 [7.6-11.8]	14
Platelet Count, 1st Research Draw	170 [13-581]	15	152 [70-537]	14
Platelet Count, Nadir	140 [37-578]	16	134 [33-194]	14
White Blood Cell Count, 1st Research Draw	10.0 [1.1-24.2]	15	11.0 [2.2-29.8]	14
Polymorphonuclear Cell Count, Absolute, 1st Research Draw	7.8 [0.2-21.3]	15	10.3 [2.0-25.8]	14
Lymphocyte Count, Absolute, 1st Research Draw	1.8 [0.4-5.3]	15	0.9 [0.1-5.7]	14
Monocyte Count, Absolute, 1st Research Draw	0.5 [0.0-1.9]	15	0.2 [0.0-1.4]	14
Eosinophil Count, Absolute, 1st Research Draw	0.0 [0.0-0.3]	15	0.0 [0.0-0.4]	14
Basophil Count, Absolute, 1st Research Draw	0.0 [0.0-0.1]	15	0.0 [0.0-0.1]	14
Lymphocyte Count, Absolute, Nadir	0.9 [0.1-2.8]	16	0.4 [0.1-1.5]	14
Sodium, Nadir	137 [130-144]	15	131 [126-140]	14
D-Dimer, Peak	1.9 [0.2-37.4]	10	4.9 [1.2-48.0]	13
Ferritin, Peak	217 [60-16973]	7	892 [253-3868]	13
Lactate Dehydrogenase, Peak	2874 [564-15390]	5	864 [457-2761]	12
Troponin, Peak	0.1 [0.0-1.8]	4	0.6 [0.0-7.4]	13
Procalcitonin, Peak	17.62 [0.07-200.00]	8	10.04 [0.24-200.00]	11
Non-Cardiac C-Reactive Protein, Peak	21.4 [0.7-60.1]	13	26.2 [6.8-40.0]	14

*Values are expressed as counts (with percent of total) for discrete data or as medians [with range] for continuous data.
**N is the number of patients with non-missing annotation for each variable.

Supplementary Table S1: Patient Characteristics

VENDOR	CAT#	ANTIBODY/DYE and TARGET	CLONE	DILUTION
BD OptiBuild	740298	BUV395 mouse anti-human CD45RA	HI100	800
BD Horizon	612943	BUV496 mouse anti-human CD8	RPA-T8	400
BD Horizon	612916	BUV563 mouse anti-human CD19	SJ25C1	200
BD OptiBuild	751572	BUV615 mouse anti-human CD16	3G8	200
BD Horizon	612969	BUV661 mouse anti-human CD38	HIT2	400
BD Horizon	612829	BUV737 mouse anti-human CD27	L128	100
BD Horizon	612905	BUV805 mouse anti-human CD20	2H7	800
Biolegend	329920	BV421 mouse anti-human CD279 (PD-1)	EH12.2H7	100
BD Horizon	566138	BV480 mouse anti-human IgD	IA6-2	50
Tombo	13-0870-T500	Ghost Dye™ Violet 510	NA	400
Biolegend	300436	BV570 mouse anti-human CD3	UCHT1	25
Biolegend	356520	BV605 mouse anti-human CD138 (Syndecan-1)	MI15	25
Biolegend	305642	BV650 mouse anti-human CD95 (Fas)	DX2	100
BD Horizon	563163	BV711 mouse anti-human CD21	B-ly4	800
BD Horizon	566355	BV750 mouse anti-human CD4	SK3	20000
BD Horizon	564041	BV786 mouse anti-human HLA-DR	G46-6	100
BD Horizon	564624	BB515 rat anti-human CD185 (CXCR5)	RF8B2	50
BD Horizon	566437	BB700 rat anti-human CD197 (CCR7)	3D12	50
BD Biosciences	CUSTOM	BB790 Strepavidin	NA	400
Biolegend	341617	Biotin rat anti-human CX3CR1	2A9-1	100
Miltenyi	130-120-716	PE recombinant anti-human TOX	REA473	50
Invitrogen	61-4877-42	PE-eFluor610 mouse anti-human EOMES	WD1928	100
Invitrogen	GRB18	PE-Cy5.5 mouse anti-human Granzyme B	GB11	2000
Biolegend	644824	PE-Cy7 mouse anti-human T-bet	4B10	800
ThermoFisher	15-9949-82	PE-Cy5 hamster anti-human CD278 (ICOS)	C398.4A	50
CellSignalingTechnology	6709S	AF647 rabbit anti-human TCF1/TCF7	C63D9	100
BD Horizon	561277	AF700 mouse anti-human Ki-67	B56	200
Biolegend	328230	APC/Fire750 anti-human CD39	A1	50

Supplementary Table 2: Panel for Peripheral Blood Mononuclear Cell Flow Cytometric Staining

VENDOR	CAT#	ANTIBODY/DYE and TARGET	CLONE	DILUTION
BD Horizon	564071	BUV395 mouse anti-human Ki67	B56	200
BD Horizon	564804	BUV496 mouse anti-human CD8	RPA-T8	500
BD Horizon	565702	BUV563 mouse anti-human CD45RA	HI100	500
BD Horizon	565069	BUV661 mouse anti-human CD38	HIT2	400
BD Horizon	564385	BUV737 mouse anti-human CD25	2A3	200
BD Horizon	565515	BUV805 mouse anti-human CD3	UCHT1	125
Biolegend	329920	BV421 mouse anti-human CD279 (PD-1)	EH12.2H7	83.3
BD Horizon	566141	BV480 mouse anti-human CD14	MP9	500
Invitrogen	L34957	LIVE/DEAD™ Fixable Aqua Dead Cell Stain Kit	NA	15000
Biolegend	318330	BV570 mouse anti-human CD56	HCD56	200
BD Horizon	562845	BV605 mouse anti-human HLA-DR	G46-6	250
Biolegend	302828	BV650 mouse anti-human CD27	O323	200
Biolegend	302044	BV711 mouse anti-human CD16	3G8	666.7
BD OptiBuild	747111	BV750 rat anti-human CD185 (CXCR5)	RF8B2	500
Biolegend	302240	BV785 mouse anti-human CD19	HIB19	125
BD Horizon	555401	FITC mouse anti-human CD15	HI98	50
BD OptiBuild	746472	BB700 mouse anti-human CD103	Ber-ACT8	500
BD Biosciences	CUSTOM	BB790 mouse anti-human CD4	SK3	1250
BD OptiBuild	746472	PE mouse anti-human CD123	9F5	400
BD Horizon	562397	PE-CF594 mouse anti-human CD127	HIL-7R-M21	200
Biolegend	310908	PE-Cy5 mouse anti-human CD69	FN50	500
eBioscience	35-0114-82	PE-Cy5.5 mouse anti-human CD11c	N418	100
Biolegend	354912	PE-Cy7 mouse anti-human CD21	BU32	2000
BD Horizon	550968	APC mouse anti-human CD161	DX12	10
BD Horizon	560566	AF700 mouse anti-human CD45	HI30	83.3
Biolegend	353212	APC-Cy7 mouse anti-human CD197 (CCR7)	G043H7	66.7

Supplementary Table 3: Lineage Panel for Whole Blood Flow Cytometric Staining

Supplemental Figure 1

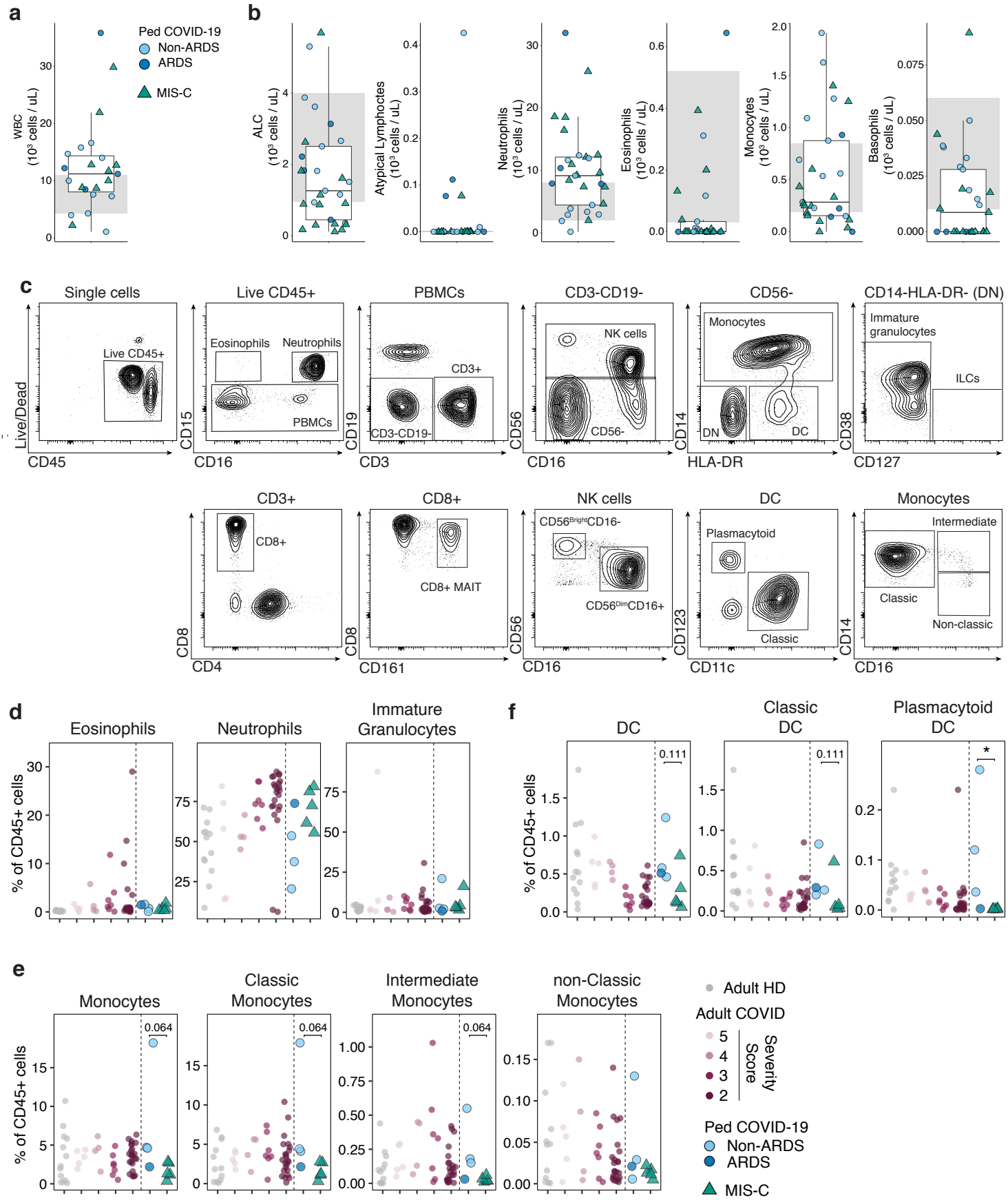

Supplemental Figure 2

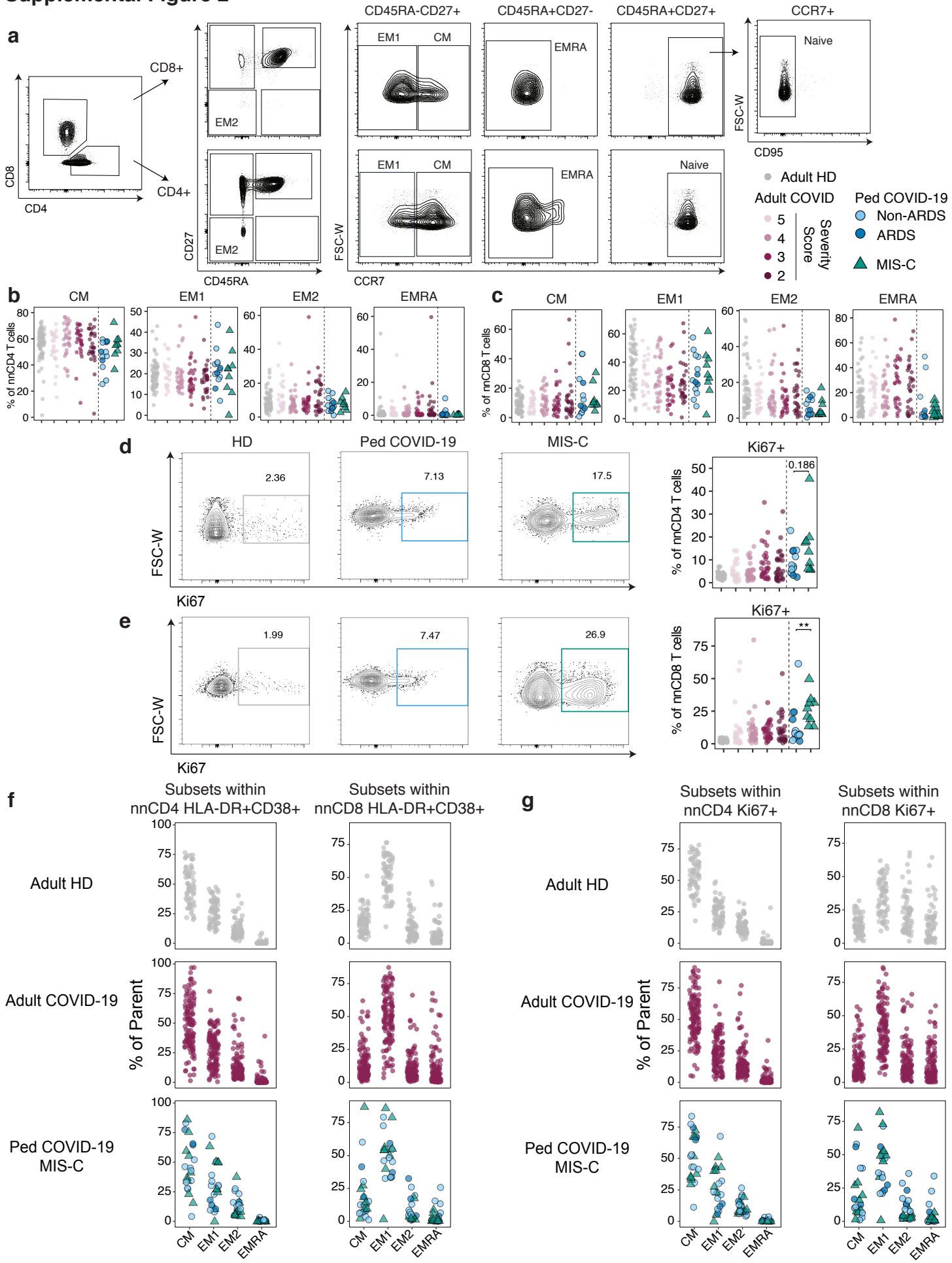

Supplemental Figure 3

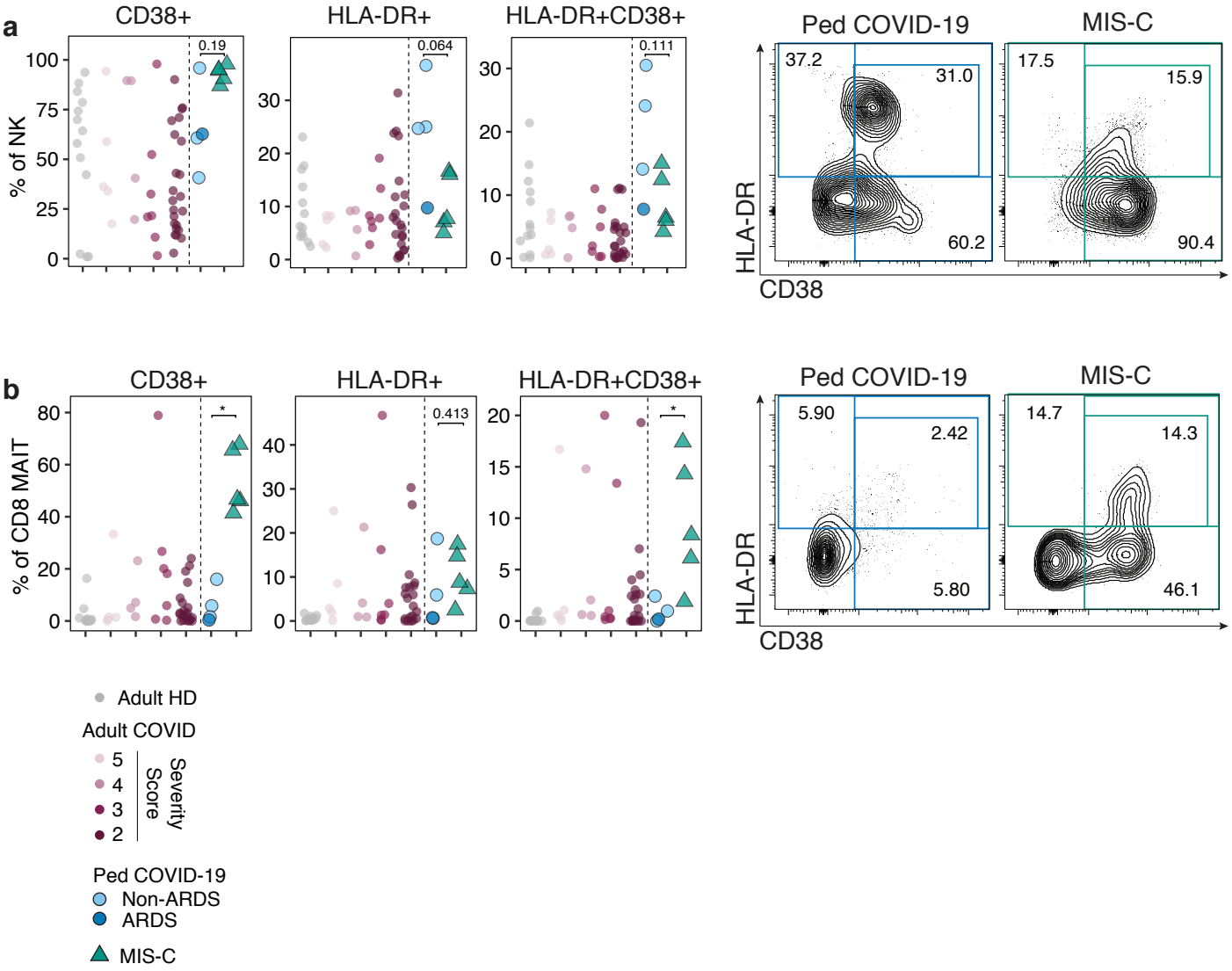

Supplemental Figure 4

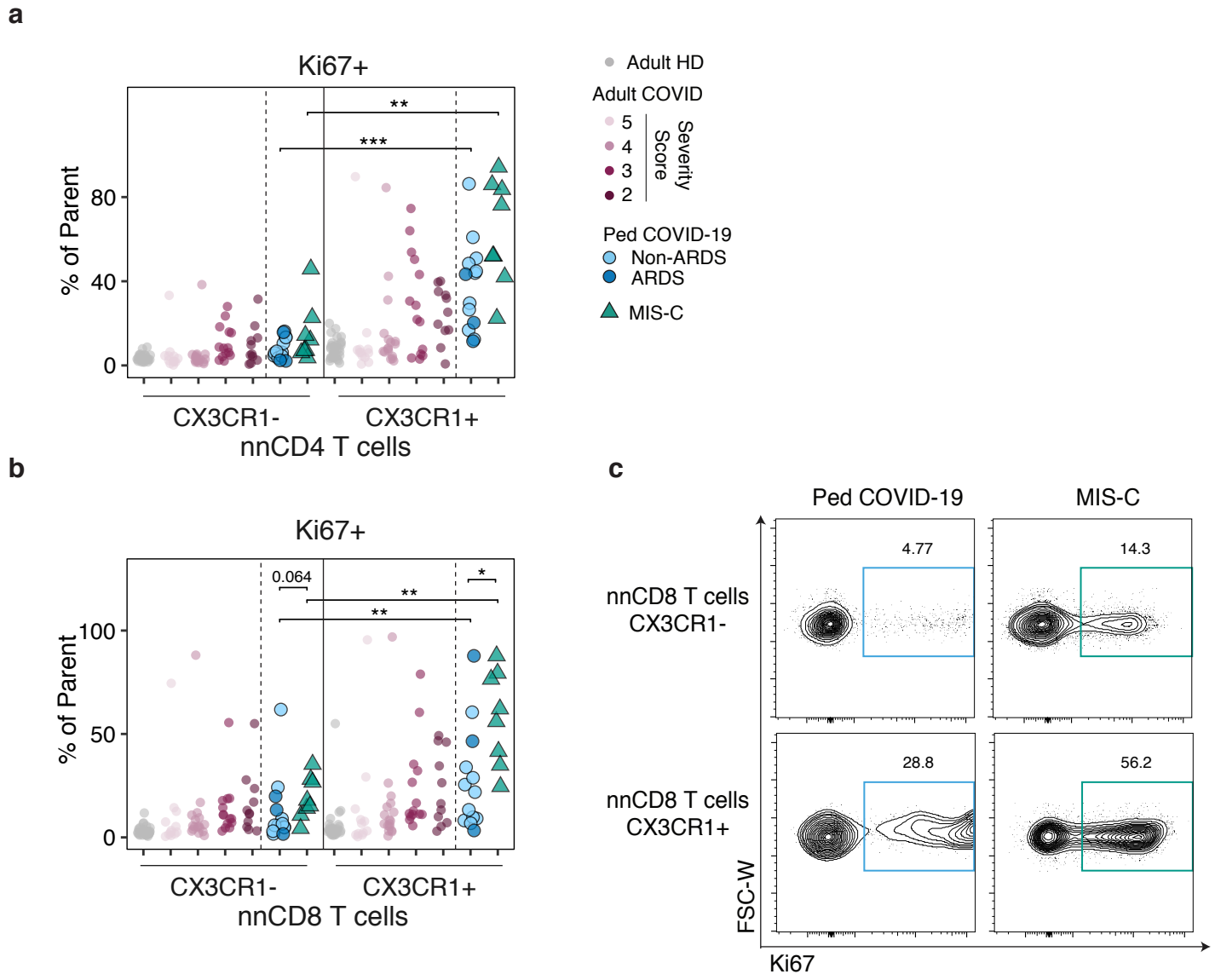

Supplemental Figure 5

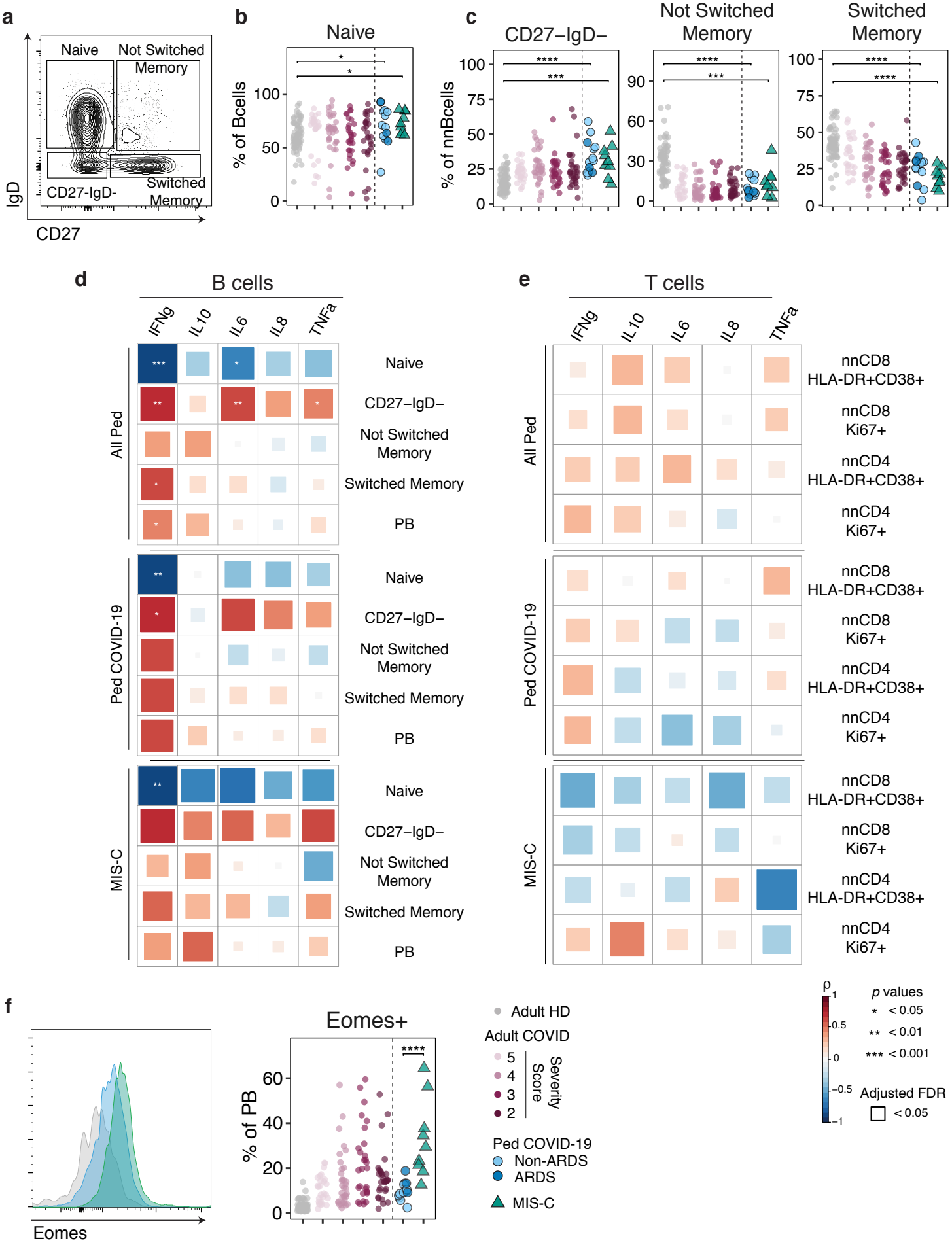

Supplemental Figure 6

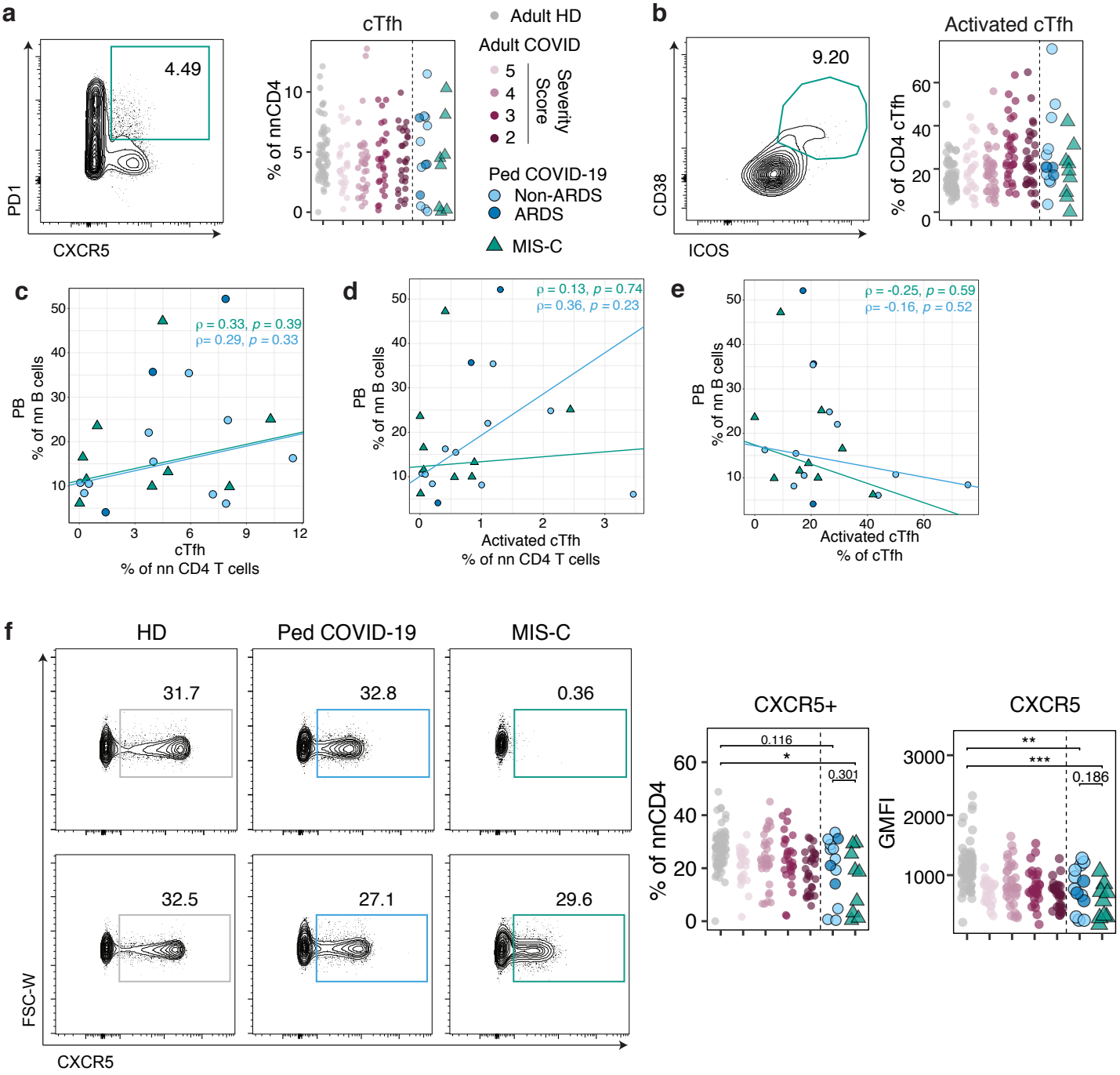

Supplemental Figure 7